Optimized Transport Properties in Lithium Doped Black Phosphorus Transistors

Tingting Gao, Xuefei Li, Xiong Xiong, Mingqiang Huang, Tiaoyang Li, and Yanqing Wu

***Abstract*— Achieving low contact resistance is one of the main challenges for black phosphorus (BP) transistors for both electronic and optoelectronic applications. Here we demonstrate a novel yet feasible lithium doping technique, which greatly reduces the contact resistance from 2 to 0.85 kΩ · μm and results in more than 2.5 times improvement in output current and ON/OFF ratio. This can be mainly attributed to the high hole doping density by lithium bis(trifluoromethylsulfonyl)-imide, which results in a narrower carrier injection barrier at the source end. The ON/OFF ratios of BP field-effect transistors with contact doping at 300 and 20 K are 432 and 7.2×10^5, respectively. A high drain current of 773 μA/μm with a 0.56 μm channel length at 20 K is also demonstrated. The doping technique provides a valid way to improve the overall performance of BP transistors.**

***Index Terms*— Molecular doping, black phosphorus, contact resistance, transistors.**

I. Introduction

BLACK phosphorus (BP) has attracted tremendous research interest due to its novel electronic properties with a tunable bandgap from 0.3-2 eV [1], [2]. Extensive work has been done on charge transport properties of few-layer BP in recent years [1]–[3]. However, the contact between commonly used metal and BP typically forms a Schottky barrier and becomes the main performance limiting factor, especially for ultrashort channel transistors [4]. Recently, surface charge transfer method has been utilized to effectively dope the two-dimensional semiconductor materials including BP and MoS_2 [5], [6]. This doping mechanism involves charge transfer at the interface between the semiconductor and surface dopants due to the large work-function/electronegativity difference, which results in spontaneous injection of electrons/holes [7]. While the dopants adsorbed on the channel surface lead to the enhancement of the on-state current, the main drawback is that they usually cause threshold voltage shift toward early turning-on with a smaller on/off ratio [5], [6]. As a result, in addition to the channel doping, it is highly important to develop new doping methods to improve the on-state current and on/off ratio simultaneously for BP transistors.

In this work, we present a novel lithium molecular doping method on the BP material. Specifically, we demonstrate a two-step doping technique to improve the on-state current and on/off ratio of BP FETs at the same time. The first step focuses on the contact interface between the metal and BP in the source/drain area (contact doping). The second step is the channel surface of BP (channel doping). After this two-step doping process, a reduction of R_c from 2 kΩ · μm to 0.85 kΩ · μm, 2.5 times increase in on current, as well as 2.7 times improvement in the on/off ratio can be achieved in the BP transistors. In addition, a saturation velocity of 7.6×10^6 cm/s has been demonstrated. Our results open up a new approach for low R_c and high-performance devices based on two-dimensional BP materials for future electronic and optoelectronic applications.

II. Device Fabrication And Characterization

Few-layer BP flakes were obtained using mechanical exfoliation onto a 30-nm atomic layer deposited $HfSiO_x$/Si substrate. The capacitance of the 30-nm $HfSiO_x$ dielectric is ~0.53 μF/cm^2 and the dielectric constant is approximately 18. Source/drain electrodes were patterned by electron-beam (e-beam) lithography and Ni (20 nm)/Au (60 nm) metal contact was deposited by e-beam evaporation. First, we studied the effect of channel doping, where the dopant was on the channel surface of BP devices only. The fabricated sample was soaked in an isopropyl alcohol solution of 0.4 mmol/L Li-TFSI for 30 min, followed by a spin-drying cycle at 2,000 rpm for 10 s. Next, we explored contact doping during the fabrication of the device. The dopant was introduced right after the lithography step of source/drain contacts. Isopropyl alcohol solution of 0.25 mmol/L Li-TFSI was spin-coated onto the device at 2,000 rpm for 10 s and contact metal was then deposited immediately. After electrical measurement of the device with contact doping, channel doping process was applied again on the same device as global doping. The electrical properties of BP devices were characterized from 300 to 20 K under vacuum ($\leq 10^{-5}$ Torr).

Fig. 1a shows the schematic structures of the BP back-gate FETs. Lithium bis(trifluoromethanesulfonyl)imide (Li-TFSI) was used for three kinds of doping schemes including the channel doping, contact doping, and global doping which includes both of the contact and channel doping. Fig. 1a also shows the molecular structure of the dopant Li-TFSI which

Manuscript received March 6, 2018; accepted March 25, 2018. Date of publication March 29, 2018; date of current version April 24, 2018. This work was supported by the National Natural Science Foundation of China under Grant 61574066 and Grant 61390504. The review of this letter was arranged by Editor M. Passlack. *(Corresponding author: Yanqing Wu.)*

The authors are with the Wuhan National High Magnetic Field Center and the School of Optical and Electronic Information, Huazhong University of Science and Technology, Wuhan 430074, China (e-mail: yqwu@mail.hust.edu.cn).

Color versions of one or more of the figures in this letter are available online at http://ieeexplore.ieee.org.

Digital Object Identifier 10.1109/LED.2018.2820841

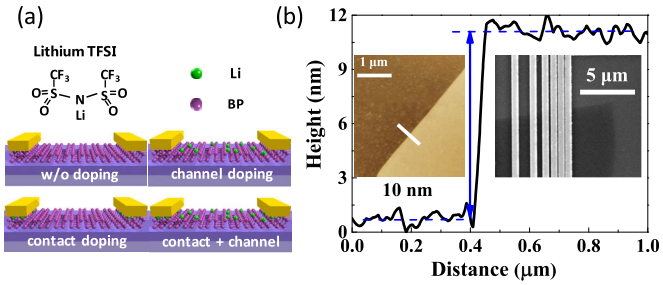

Fig. 1. (a) Schematic view of the device fabricated in this work. Three different approaches for Li-doped few-layer BP back-gate FET: channel, contact, and contact plus channel doping. (b) Thickness measured by atomic force microscopy of BP flake is 10 nm. Inset: AFM image of the BP flake and a SEM image of BP FETs with different channel lengths.

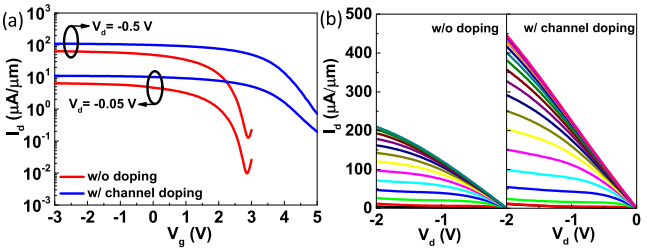

Fig. 2. (a) Transfer characteristics of the few-layer BP FETs of 0.56 μm channel length with and without channel doping. (b) Output characteristics of the BP FETs before and after channel doping. The drain current improves significantly by the channel doping.

serves as the source of Li^+ and was previously widely used to increase the conductivity of hole transport layer in perovskite solar cells [8], [9]. The thickness of the BP flakes used here is around 10 nm as shown in the atomic force microscopy image in Fig. 1b. We fabricated the devices with channel length from 1 μm to 0.1 μm as shown in the inset of Fig. 1b, which were then used to extract contact resistance by transfer length method.

III. Results And Discussion

To investigate the effect of Li-TFSI channel doping, direct current (DC) transfer characteristics of a representative 0.56-μm long BP FET before and after doping at 300 K are shown in Fig. 2a. The threshold voltage (V_{th}) of devices before and after Li doping extracted by linear extrapolation method using transfer characteristics is 2.5 V and 4.5 V, respectively. The increased carrier density due to the channel doping is estimated to be approximately 6.3×10^{12} /cm^2 according to the equation: $n = C_{ox} * \Delta V_{th}/q$, where C_{ox} is the capacitance of the gate dielectric, q is the electrostatic constant, and ΔV_{th} is the value of threshold voltage shift. Devices with different channel lengths before and after Li doping are measured, exhibiting the same positive V_{th} shift. The effective field-effect mobility of the BP FET before and after Li doping is estimated to be about 104 and 147 cm^2/(V·s), respectively [10]. The on/off ratio of the undoped BP FET is 653 and reduces to 55 after doping. This degradation in on/off ratios has frequently been observed in other 2D materials after the channel doping, which can be mainly attributed to the weaker electrostatic control of the channel by the back gate and the increased leakage current through the doping layer [5], [7] Fig. 2b compares the output characteristics of BP FET with and without Li channel doping. The maximum on-current of the BP FET without doping at $V_{\text{d}} = -2$ V is 210 μA/μm and increases to 450 μA/μm after doping, showing that Li channel doping can effectively enhance the on-state performance of BP transistors. Meanwhile, the channel doping can be removed by repeated soaking and rinsing the sample in the isopropyl alcohol.

In order to improve the on/off ratio, contact doping is adopted in a similar fashion as the channel doping where Li-TFSI is applied to the interface between the BP and the contact metal in the source/drain area. The increased carrier density due to the contact doping is estimated to be 3.9×10^{12} /cm^2. Transfer characteristics of a 0.56 μm BP FETs with and without contact doping at 300 and 20 K are shown in Fig. 3a. For the undoped BP devices, the on/off ratios at 300 and 20 K are 100 and 580, respectively. After contact doping with the Li-TFSI molecule, the transfer characteristics change drastically with the improved on/off ratio of 432 and 7.2×10^5 at 300 and 20 K, respectively. The on-current improves more than 2 times, along with the great reduction of the off-state current especially at low temperature. The off current is determined by a thermionic barrier for holes to transfer from source to channel. After contact doping, the Fermi level of BP shifts toward the valence band and results in a larger band bending with respect to the channel, which is in the p-type depletion region [11]. Hence, the off-current decreases after contact doping accordingly. As shown in Fig. 3b, extrinsic g_{m} of BP devices increases about 2 and 4 times after contact doping at 300 and 20 K, respectively. Fig. 3c and 3d show the output characteristics the BP FET without and with contact doping at 20 K, respectively. The drain current increases from 304 μA/μm to 773 μA/μm after Li contact doping. Fig. 3e and 3f show the output characteristics of the BP FET with contact doping and global doping at 300 K, respectively. The drain current increases from 433 μA/μm to 492 μA/μm after Li global doping. The I_{d}-V_{d} curves are consistent over the time during the measurement under vacuum and are repeatable after large current flow, indicating a good stability. The enhancement in on/off ratios, g_{m}, and drain current shows that overall improvement in the electrical transport can be obtained in contact doped BP FETs. Moreover, this doping approach can be further applied to a wide range of the typically non-alloyed contact in 2D devices. The long-term stability of the doped BP transistors in air is mainly limited by the BP channel. It has been revealed that Al_2O_3 from a thin Al layer deposited by physical vapor deposition (PVD) can be used to passivate the BP devices, which has shown significantly improved air stability without performance degradation up to 6 weeks in ambient conditions, which can also be potentially used to encapsulate doped regions [12].

Fig. 4a and 4b show the off current and on/off ratio of BP devices as a function of temperature before and after contact and global doping, respectively. It is clear that the off current decreases at lower temperatures and the on/off ratio increases monotonically with the decreasing temperature from 300 to 20 K. The on/off ratio of the BP FET with

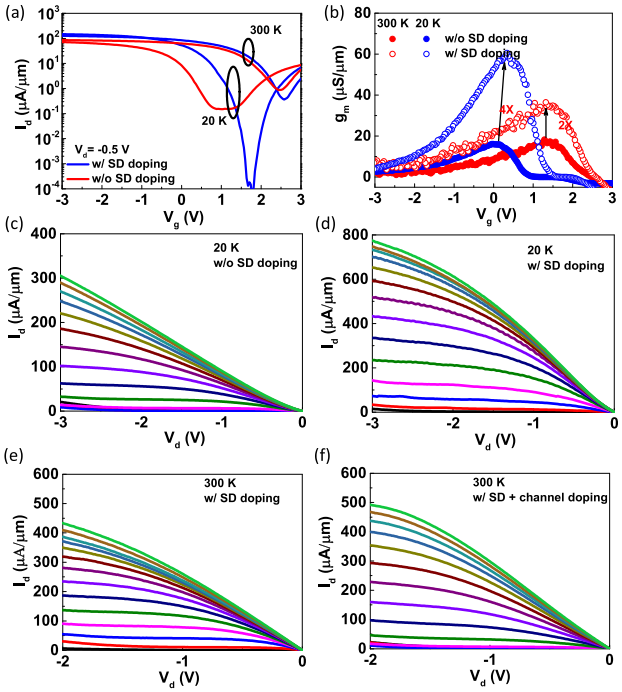

Fig. 3. (a) Transfer characteristics of the few-layer BP FETs of 0.56 μm channel length with and without contact doping at 300 and 20 K. (b) Maximum transconductance of the BP devices at $V_{\rm d} = -0.5$ V. Output characteristics of the few-layer BP FETs by Li-TFSI at 20 K (c) without contact doping and (d) with contact doping. Output characteristics of the few-layer BP FETs at 300 K (e) with contact doping and (f) global doping.

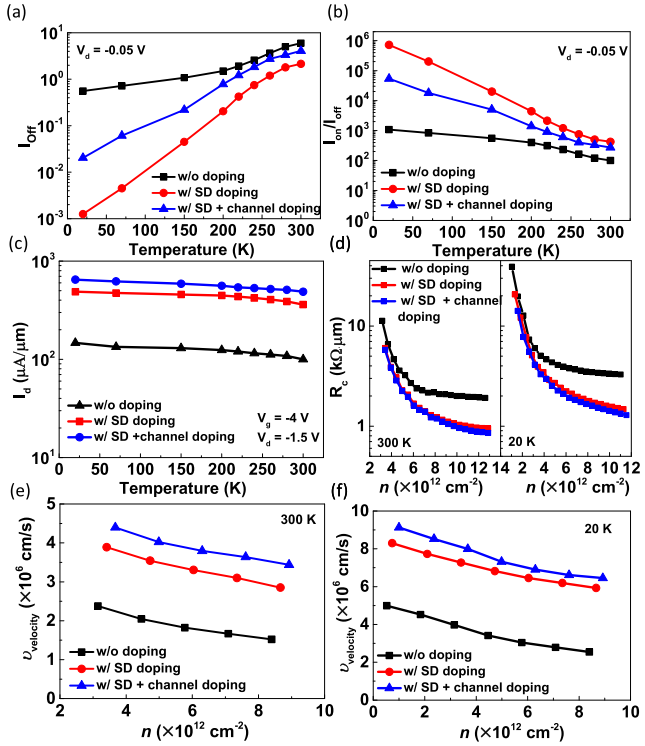

Fig. 4. Temperature dependent (a) Off current, (b) I_{ON}/I_{OFF} ratio, and (c) drain current for various doping schemes for a 0.56-μm channel device. (d) Contact resistance as a function of carrier density for the same devices in Fig. 4(a) at 300 and 20 K. Carrier drift velocity of the 0.16-μm BP FETs with and without Li doping (e) at 300 K and (f) 20 K.

contact doping is always larger than that of the undoped one, consistent with the results in Fig. 3a. It should be noted that channel doping could decrease the on/off ratios slightly in the global doping approach. The sub-threshold swings (SS) of BP FETs derived from the p-branch without doping, with contact doping, and global doping at 300 K are 0.60 V/dec, 0.39 V/dec and 0.52 V/dec, respectively. The improved SS in the contact doping case can also be attributed to the higher barrier of holes between source and channel at subthreshold region. The corresponding maximum on-current comparison is presented in Fig. 4c. As expected, the BP FET with the global doping exhibits the highest drain current at all temperatures. We can extract the $R_{\rm c}$ using transfer length method according to the equation: $R_{tatal} = 2R_c + R_s\frac{L}{W}$, where $R_{\rm total}$ is the total resistance, $R_{\rm c}$ is contact resistance, $R_{\rm s}$ is sheet resistance, L is channel length, and W is channel width [5], [13]. As shown in Fig. 4d, the decrease of $R_{\rm c}$ at larger gate bias can be attributed to the increase of electrostatic doping by the back gate [4], [13]. At $V_{\rm g} = -4$ V, the $R_{\rm c}$ of BP FETs before and after global doping are 2 k$\Omega \cdot \mu$m and 0.85 k$\Omega \cdot \mu$m, respectively. This improvement in $R_{\rm c}$ can be attributed to the high hole doping density induced by Li-TFSI which facilitates the hole injection from the metal into the valence band of BP [4], [14] Therefore, this result shows that the contact doping method is an effective approach to reduce the contact resistance and improve the drain current as well as on/off ratio, which are desirable for high performance BP FETs. Furthermore, we extract carrier drift velocity at 300 and 20 K using the formula $\upsilon = I_d/WC_{ox}(V_g - 2I_dR_c - V_{th})$ as shown in Fig. 4e and 4f, respectively [15], [16]. The $R_{\rm c}$ values used for drift velocity calculation in the global doping, SD doping, and without doping at 20 K are 1.5, 1.8, and 3.4 k$\Omega \cdot \mu$m, respectively. The maximum drift velocity of the undoped device at 300 K and 20 K are 3.0×10^6 cm/s 4.2×10^6 cm/s at $V_{\rm d} = -3.5$ V, respectively, which is comparable to previous results [17]. The drift velocity increases by a factor of 1.6 after contact doping, and reaches to 7.6×10^6 cm/s after the global doping at 20 K. The improvement in drift velocity is mainly attributed to both increased extrinsic mobility and effective electric field in the channel [5].

IV. Conclusion

In summary, we have investigated the effect of Li-TFSI doping on the electrical properties of BP FETs. The overall performance of BP FETs can be improved with 2.3 times decrease in contact resistance, 2.7 times improvement in the on/off ratio and 2.5 times improvement in drain current. Moreover, the carrier drift velocity at 20 K reaches to around 7.6×10^6 cm/s. Meanwhile, this doping technique is useful to reduce access resistance and minimize the parasitic effects in the high-frequency operation of BP radio frequency (RF) transistors. The contact doping can improve the on/off ratio, which is critical to a high-power gain in RF devices. The global doping can increase $g_{\rm m}$, which is in favor of improving the cut off frequency. These improvements of the key figures of merit show great potential of high-performance BP in future high-speed electronic and optoelectronic applications.

REFERENCES

[1] L. Li, Y. Yu, G. J. Ye, Q. Ge, X. Ou, H. Wu, D. Feng, X. H. Chen, and Y. Zhang, "Black phosphorus field-effect transistors," *Nature Nanotech.*, vol. 9, pp. 372–377, Mar. 2014, doi: 10.1038/nnano.2014.35.

[2] H. Liu, A. T. Neal, Z. Zhu, Z. Luo, X. Xu, D. Tománek, and P. D. Ye, "Phosphorene: An unexplored 2D semiconductor with a high hole mobility," *ACS Nano*, vol. 8, no. 4, pp. 4033–4041, Mar. 2014, doi: 10.1021/nn501226z.

[3] F. Xia, H. Wang, and Y. Jia, "Rediscovering black phosphorus as an anisotropic layered material for optoelectronics and electronics," *Nature Commun.*, vol. 5, Jul. 2014, Art. no. 4458, doi: 10.1038/ncomms5458.

[4] Y. Du, H. Liu, Y. Deng, and P. D. Ye, "Device perspective for black phosphorus field-effect transistors: Contact resistance, ambipolar behavior, and scaling," *ACS Nano*, vol. 8, no. 10, pp. 10035–10042, Oct. 2014, doi: 10.1021/nn502553m.

[5] Y. Du, L. Yang, H. Zhou, and P. D. Ye, "Performance enhancement of black phosphorus field-effect transistors by chemical doping," *IEEE Electron Device Lett.*, vol. 37, no. 4, pp. 429–432, Apr. 2016, doi: 10.1109/LED.2016.2535905.

[6] D. Kiriya, M. Tosun, P. Zhao, J. Kang, and A. Javey, "Air-stable surface charge transfer doping of MoS_2 by benzyl viologen," *J. Am. Chem. Soc.*, vol. 136, no. 22, pp. 7853–7856, May 2014, doi: 10.1021/ja5033327.

[7] X. Zhang, Z. Shao, X. Zhang, Y. He, and J. Jie, "Surface charge transfer doping of low-dimensional nanostructures toward high-performance nanodevices," *Adv. Mater.*, vol. 28, no. 47, pp. 10409–10442, Dec. 2016, doi: 10.1002/adma.201601966.

[8] H. Snaith and M. Grätzel, "Enhanced charge mobility in a molecular hole transporter via addition of redox inactive ionic dopant: Implication to dye-sensitized solar cells," *Appl. Phys. Lett.*, vol. 89, no. 26, p. 262114, Nov. 2006, doi: 10.1063/1.2424552.

[9] E. J. Juarez-Perez, M. R. Leyden, S. Wang, L. K. Ono, Z. Hawash, and Y. Qi, "Role of the dopants on the morphological and transport properties of Spiro-MeOTAD hole transport layer," *Chem. Mater.*, vol. 28, no. 16, pp. 5702–5709, Jul. 2016, doi: 10.1021/acs.chemmater.6b01777.

[10] X. Li, L. Yang, M. Si, S. Li, M. Huang, P. D. Ye, and Y. Wu, "Performance potential and limit of MoS_2 transistors," *Adv. Mater.*, vol. 27, no. 9, pp. 1547–1552, Mar. 2015, doi: 10.1002/adma.201405068.

[11] H. Fang, S. Chuang, T. C. Chang, K. Takei, T. Takahashi, and A. Javey, "High-performance single layered WSe_2 p-FETs with chemically doped contacts," *Nano Lett.*, vol. 12, no. 7, pp. 3788–3792, Jun. 2012, doi: 10.1021/nl301702r.

[12] M. Huang, S. Li, Z. Zhang, X. Xiong, X. Li, and Y. Q. Wu, "Multifunctional high-performance van der Waals heterostructures," *Nature Nanotech.*, vol. 12, no. 12, pp. 1148–1154, Oct. 2017, doi: 10.1038/nnano.2017.208.

[13] X. Li, Y. Du, M. Si, L. Yang, S. Li, T. Li, X. Xiong, P. D. Ye, and Y. Wu, "Mechanisms of current fluctuation in ambipolar black phosphorus field-effect transistors," *Nanoscale*, vol. 8, no. 6, pp. 3572–3578, Jun. 2016, doi: 10.1039/C5NR06647F.

[14] L. Yang, K. Majumdar, H. Liu, Y. Du, H. Wu, M. Hatzistergos, P. Hung, R. Tieckelmann, W. Tsai, C. Hobbs, and P. D. Ye, "Chloride molecular doping technique on 2D materials: WS_2 and MoS_2," *Nano Lett.*, vol. 14, no. 11, pp. 6275–6280, Oct. 2014, doi: 10.1021/nl502603d.

[15] K. Lam, Z. Dong, and J. Guo, "Performance limits projection of black phosphorous field-effect transistors," *IEEE Electron Device Lett.*, vol. 35, no. 9, pp. 963–965, Sep. 2014, doi: 10.1109/LED.2014.2333368.

[16] V. E. Dorgan, A. Behnam, H. J. Conley, K. I. Bolotin, and E. Pop, "High-field electrical and thermal transport in suspended graphene," *Nano Lett.*, vol. 13, no. 10, pp. 4581–4586, Feb. 2013, doi: 10.1021/nl400197w.

[17] W. Zhu, S. Park, M. N. Yogeesh, K. M. McNicholas, S. R. Bank, and D. Akinwande, "Black phosphorus flexible thin film transistors at gighertz frequencies," *Nano Lett.*, vol. 16, pp. 2301–2306, Mar. 2016, doi: 10.1021/acs.nanolett.5b04768.